Vector transmission matrix for the polarization behavior of light propagation in highly scattering media

Santosh Tripathi,[1] Richard Paxman,[2] Thomas Bifano,[3] and Kimani C. Toussaint, Jr.[4,*]

[1] *Department of Electrical and Computer Engineering, University of Illinois at Urbana-Champaign, 1406, W. Green St., Urbana, Illinois 61801, USA*
[2] *Paxman Consulting, 9228 Sunset Lake Dr., Saline, Michagan 48176, USA*
[3] *Boston University Photonics Center, 8 Saint Marys St., Boston, Massachusetts 02215, USA*
[4] *Department of Mechanical Science and Engineering, University of Illinois at Urbana-Champaign, 1206, W. Green St., Urbana, Illinois 61801, USA*

[*] *ktoussai@illinois.edu*

Abstract: Recently the optical transmission matrix (TM) has been shown to be useful in controlling the propagation of light in highly scattering media. In this paper, we present the vector transmission matrix (VTM) which, unlike the TM, captures both the intensity and polarization transmission property of the scattering medium. We present an experimental technique for measuring the absolute values of the VTM elements which is in contrast to existing techniques whereby the TM elements are measured to within a scaling factor. The usefulness of the VTM is illustrated by showing that it can be used to both predict and control the magnitude of the complex polarization ratio of the light focused through the scattering medium. To the best of our knowledge, this is the first study to show the possibility of controlling the polarization of the light transmitted through highly scattering media.

OCIS codes: (260.5430) Polarization; (120.5410) Polarimetry; (120.0120) Instrumentation, measurement, and metrology.

References and links

1. I. M. Vellekoop and A. P. Mosk, "Focusing coherent light through opaque strongly scattering media," Opt. Lett. **32**, 2309–2311 (2007).
2. S. M. Popoff, G. Lerosey, R. Carminati, M. Fink, A. C. Boccara, and S. Gigan, "Measuring the transmission matrix in optics: an approach to the study and control of light propagation in disordered media," Phys. Rev. Lett. **104**, 100601 (2010).
3. S. Popoff, G. Lerosey, M. Fink, A. C. Boccara, and S. Gigan, "Image transmission through an opaque material," Nat. Commun. **1**, 81 (2010).
4. I. M. Vellekoop, A. Lagendijk, and A. P. Mosk, "Exploiting disorder for perfect focusing," Nat. Photonics **4**, 320–322 (2010).
5. S. M. Popoff, A. Aubry, G. Lerosey, M. Fink, A. C. Boccara, and S. Gigan, "Exploiting the time-reversal operator for adaptive optics, selective focusing, and scattering pattern analysis," Phys. Rev. Lett. **107**, 263901 (2012).
6. D. B. Conkey, A. M. Caravaca-Aguirre, and R. Piestun, "High-speed scattering medium characterization with application to focusing light through turbid media," Opt. Express **20**, 1733–1740 (2012).
7. Y. Choi, T. Yang, C. Fang-Yen, P. Kang, K. Lee, R. Dasari, M. Feld, and W. Choi, "Overcoming the diffraction limit using multiple light scattering in a highly disordered medium," Phys. Rev. Lett. **107**, 023902 (2011).
8. A. Dolginov, Y. Gnedin, and N. Silant'ev, "Photon polarization and frequency change in multiple scattering," J. Quantum Spectrosc. Ra. **10**, 707–754 (1970).

#168000 - $15.00 USD Received 4 May 2012; revised 15 Jun 2012; accepted 16 Jun 2012; published 29 Jun 2012

9. T. Kohlgraf-Owens and A. Dogariu, "Finding the field transfer matrix of scattering media," Opt. Express **16**, 13225–13232 (2008).
10. T. Kohlgraf-Owens and A. Dogariu, "Transmission matrices of random media: Means for spectral polarimetric measurements," Opt. Lett. **35**, 2236–2238 (2010).
11. C. Prada and M. Fink, "Eigenmodes of the time reversal operator: A solution to selective focusing in multiple-target media," Wave Motion **20**, 151–163 (1994).
12. C. Prada and J.-L. Thomas, "Experimental subwavelength localization of scatterers by decomposition of the time reversal operator interpreted as a covariance matrix," J. Acoust. Soc. Am. **114**, 235–243 (2003).
13. J. Pasquesi, S. Schlachter, M. Boppart, E. Chaney, S. Kaufman, and S. Boppart, "In vivo detection of exercise-induced ultrastructural changes in genetically-altered murine skeletal muscle using polarization-sensitive optical coherence tomography," Opt. Express **14**, 1547–1556 (2006).
14. R. Rao, M. Mehta, and K. Toussaint Jr., "Fourier transform-second-harmonic generation imaging of biological tissues," Opt. Express **17**, 14534–14542 (2009).
15. C. Krafft, B. Dietzek, and J. Popp, "Raman and cars microspectroscopy of cells and tissues," Analyst **134**, 1046–1057 (2009).
16. B. E. A. Saleh and M. C. Teich, *Fundamentals of Photonics* (John Wiley and Sons, 2007).
17. R. C. Gonzalez and R. E. Woods, *Digital Image Processing* (Prentice Hall, 2007).
18. B. Schaefer, E. Collett, R. Smyth, D. Barrett, and B. Fraher, "Measuring the stokes polarization parameters," Am. J. Phys. **75**, 163–168 (2007).
19. R. H. Byrd, J. Nocedal, and R. A. Waltz, "Knitro: An integrated package for nonlinear optimization," in *Large Scale Nonlinear Optimization,* G. D. Pillo and F. Giannessi, eds. (Springer Science+Business Media, 2006).

1. Introduction

The ability to control the transmission of light through a highly scattering medium (HSM) has a multitude of potential applications and has recently garnered special attention [1–7]. In 2007 it was shown that light can be focused through an HSM by iteratively adjusting the phase profile of the field incident on it [1]. The study was later systematized in 2010 by the introduction of the concept of the transmission matrix (TM), each element of which relates the transmission of an optical field from an incident to an observation point [2]. Since then the ability to focus light through disordered media has been put to use in a variety of interesting applications such as 'sub-diffraction' imaging [4] and image transmission through an HSM [3]. A recent trend towards using high-speed spatial light modulators for the focusing problem is bound to further enable a large number of new and exciting applications and developments [5,6]. However, although the effect of multiple scattering on the polarization of the scattered light has been investigated for some time [8–10], the control of the polarization state for light transmitted through an HSM has heretofore not been explored. With optical fields, in many cases, the intensity is the only parameter of concern. However, there are many important applications where polarization plays a crucial role and warrants consideration. For example, being able to control the polarization of the light transmitted thorough the HSM could extend the capabilities of polarization sensitive deep-tissue imaging techniques such as polarization-sensitive optical coherence tomography [13] as well as various coherent nonlinear microscopy techniques (eg., SHG [14] and CARS [15]). It could also be useful in imaging the dipole orientation of the molecules immobilized in a matrix for single molecule studies, and for the curing of polarization sensitive polymers in 3D fabrication.

In this paper, we generalize the concept of the TM used in the experiments controlling the light propagation through an HSM [2,6] to take into account the polarization of optical fields resulting in the vector transmission matrix (VTM). Further, we outline a method for measuring the absolute values of the VTM elements. It is in contrast to the TM measurements reported in the literature where the TMs have been measured upto a scaling factor [5,6]. Moreover, we show experimentally that the VTMs can be used to optimize the focus of light through an HSM as well as to predict and control the magnitude of the complex polarization ratio [16] i.e. ratio of the amplitudes along each polarization basis state of the focused light.

The paper is organized as follows. In Section 2, we present the concept of the VTM and

#168000 - $15.00 USD Received 4 May 2012; revised 15 Jun 2012; accepted 16 Jun 2012; published 29 Jun 2012

present both the theory and an experimental setup for measuring it. In Section 3, we outline a method for optimizing the polarization components of the focused optical field using the VTM. Section 4 presents the experimental results and discussion which is followed by the conclusions in the Section 5.

2. Measurement of the vector transmission matrix

It is well known that the effect of multiple scattering is to scramble the polarization of the input field [8]. However, since any polarization state can be represented as a linear combination of two orthogonal basis polarization states [16], to capture the polarization changing behavior of an HSM, it is sufficient to measure components of the output field along each of the basis polarization states as a function of the basis states at the input. Although any set of basis states can be chosen, in this paper, we take the canonical x and y polarization directions, corresponding to the horizontal and vertical direction in the laboratory reference frame as basis states. Assuming that there are $2M$ input degrees of freedom and N observation points, the VTM can be defined to relate the input and output field as

$$\begin{pmatrix} t^{xx}_{1,1} & \cdots & t^{xx}_{1,M} & t^{xy}_{1,1} & \cdots & t^{xy}_{1,M} \\ \vdots & \ddots & \vdots & \vdots & \ddots & \vdots \\ t^{xx}_{N,1} & \cdots & t^{xx}_{N,M} & t^{xy}_{N,1} & \cdots & t^{xy}_{N,M} \\ t^{yx}_{1,1} & \cdots & t^{yx}_{1,M} & t^{yy}_{1,1} & \cdots & t^{yy}_{1,M} \\ \vdots & \ddots & \vdots & \vdots & \ddots & \vdots \\ t^{yx}_{N,1} & \cdots & t^{yx}_{N,M} & t^{yy}_{N,1} & \cdots & t^{yy}_{N,M} \end{pmatrix} \begin{pmatrix} E^{x(I)}_1 \\ \vdots \\ E^{x(I)}_M \\ E^{y(I)}_1 \\ \vdots \\ E^{y(I)}_M \end{pmatrix} = \begin{pmatrix} E^{x(O)}_1 \\ \vdots \\ E^{x(O)}_N \\ E^{y(O)}_1 \\ \vdots \\ E^{y(O)}_N \end{pmatrix}, \tag{1}$$

where $E^{i(I)}_m$ represents the i polarization component at the mth input point with $i = x, y$ and $m = 1$ to M. Similarly, $E^{i(O)}_n$ represents the i polarization component at the nth observation point with $n = 1$ to N. The VTM is of size $2N \times 2M$ and its element $t^{ij}_{n,m}$ gives the contribution of the j polarization component of the field in the mth input state to i polarization component of the field on the nth observation point. The TMs reported in the literature [2,6] are a subset of the VTM shown in Eq. (1). For example, with a y polarized input field incident on an HSM and the analyzer customarily used in the TM measurements [2,6] at the output oriented along the x direction, the elements of the VTM shown in the box in Eq. (1) constitute the scalar TM measured.

Figure 1 shows the experimental setup used for VTM measurements. In the figure, a 45°-polarized continuous wave input laser beam is incident upon a non-polarizing beam splitter BS1 thereby creating a reflected and a transmitted beam. The latter then enters a polarizing beam splitter PBS which decomposes the beam into horizontally and vertically polarized components leading to beams B1 and B2, respectively. B1 and B2 are then respectively steered by mirrors M1 and M2 onto a second beam splitter BS2 which then directs both beams onto a nematic liquid crystal spatial light modulator NLC-SLM. As shown in the figure, B1 and B2 are spatially separate on the NLC-SLM which provides independent phase modulation for each of the beams. This spatial separation of the beams is achieved by walking B2 vertically by tilting PBS and M2 appropriately. Since the NLC-SLM used in our experiments provides phase modulation only for a vertically polarized optical field, B1 is converted to a vertically polarized beam by passing it through a half-wave plate HWP. The surface of the NLC-SLM

#168000 - $15.00 USD Received 4 May 2012; revised 15 Jun 2012; accepted 16 Jun 2012; published 29 Jun 2012

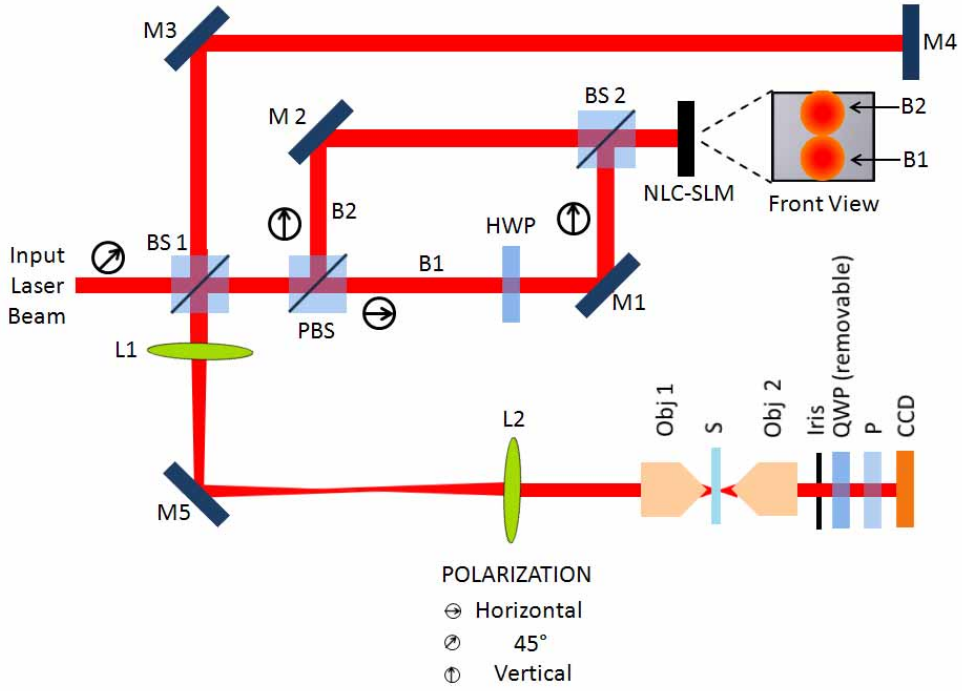

Fig. 1. Experimental setup to measure the vector transmission matrix. Refer to text for details.

is then imaged by lens pair L1 and L2 onto the back focal plane of an optical objective Obj1 which focuses the light onto the HSM sample S. The forward scattered optical field is then collected by another objective Obj2, passed through an analyzer P, and subsequently recorded by a CCD camera. This optical field recorded on the CCD is our control signal. The quarter-wave plate QWP shown in the setup is flipped out of the beam path while collecting the VTM elements and flipped into the beam path during polarization measurements. It is worth noting that the component of the scattered light recorded on the CCD that comes from the beam reflected off BS1, steered by M3 and retro-reflected by mirror M4 acts as the reference during VTM measurements. To avoid ambiguity, we define the total reference and total control signals as the reference and control signals that would be recorded by the CCD in the absence of any optical component between the Obj2 and CCD.

In our experiments the laser source was an 808-nm diode laser, IQ2C(808-150), acquired from Power Technology, Inc. Although not shown in the figure, the beam coming out of the laser module was expanded, spatially filtered and passed through a half-wave plate-polarizer combination prior to being incident on BS1. The beam splitters BS1, PBS and BS2 with respective part numbers BS013, PBS252 and BS014 were acquired from Thorlabs, Inc. The NLC-SLM is a 512×512 XY series NLC-SLM acquired from Boulder Nonlinear Systems. The HWP, QWP and P were acquired respectively from Karl Lambrecht Corporation, CVI Melles Griot and Thorlabs, Inc. with respective part numbers MWPQA2-12-V800, QWPO-800-06-4-R10 and LPNIR050-MP. The QWP and P were mounted separately on two PRM1Z8E motorized rotation mount and controller acquired from Thorlabs, Inc. and were controlled through a custom computer code written in MATLAB and LabVIEW. The camera used in our experiments was a Hamamatsu ORCA-285G. The Obj1 was an infinity corrected Spencer $10\times$ objective

#168000 - $15.00 USD Received 4 May 2012; revised 15 Jun 2012; accepted 16 Jun 2012; published 29 Jun 2012

with an NA, working distance and parfocal distance of 0.25, 9.1 mm, and 34 mm, respectively. Similarly, Obj2 was an infinity corrected 45× objective from Reichert with an NA, working distance and parfocal distance of 0.66, 0.7 mm and 34 mm, respectively. We studied two types of HSM samples. They were prepared by depositing a ZnO and ethanol mixture, and white nail polish on microscope slides.

To measure the VTM we divide the SLM into 256 segments and use half of the segments to control the x polarized component B1 and the other half to control the y polarized component B2 resulting in $M = 128$. Since the contribution of each control segment at the input to an observation point at the output is weak, using the canonical basis results in a low signal-to-noise ratio; therefore we start by measuring the VTM elements using a Hadamard basis at the input [2, 6]. As in [2], we also use four-point phase shifting interferometry. To measure the VTM elements of the form t^{yj}_{n,H_m}, where the subscript H_m in the VTM represents the mth basis element of the Hadamard basis, the analyzer transmission axis is oriented along y, whereas to measure the VTM elements of the form t^{xj}_{n,H_m} the analyzer transmission axis is oriented along x. The VTM elements with Hadamard basis at the input are converted to VTM elements with the canonical elements at the input using a standard Hadamard-to-canonical transformation [17]. These transformed VTM elements are of the form

$$T^{ij}_{n,m} = \sqrt{I^{Ri}_{n,m} I^{Si}_{n,m}}\, e^{i\triangle\phi}, \tag{2}$$

where $I^{Ri}_{n,m}$ and $I^{Si}_{n,m}$ are the i polarization components of the reference and control signals at the nth observation point, respectively, and $\triangle\phi$ is the phase of the reference signal subtracted from the phase of the control signal. A VTM element should relate the input at the mth input degree of freedom to the output at the nth observation point and as such should be independent of the reference signal; however, as can be seen from Eq. (2), the measured VTM elements are scaled by a factor $\sqrt{I^{Ri}_{n,m}}$ which depends on the reference signal. Further, $T^{xj}_{n,m}$ and $T^{yj}_{n,m}$ use the x and y components of the total reference signal as reference in the phase shifting measurements. Since the x and y components of the total reference signal can have a phase difference between them, the measured phase values for $T^{xj}_{n,m}$ and $T^{yj}_{n,m}$ have an offset between them. To use all the VTM elements together this phase offset needs to be corrected for.

In our experiments we solve both of these problems by measuring the Stokes vector $\begin{bmatrix} S^{R,0}_{n,m} & S^{R,1}_{n,m} & S^{R,2}_{n,m} & S^{R,3}_{n,m} \end{bmatrix}^\top$ for the total reference signal. The Stokes vector is measured by orientating the polarizer along x direction and measuring the value of intensity on the CCD as a function of the orientation of the QWP [18]. During these measurements a beam block is placed in front of the PBS in Fig. 1. From the Stokes vector we calculate the x and y components of the total reference signal as [16]

$$I^{Rx}_{n,m} = \frac{1}{2}\left(S^{R,0}_{n,m} + S^{R,1}_{n,m}\right) \tag{3}$$

and

$$I^{Ry}_{n,m} = \frac{1}{2}\left(S^{R,0}_{n,m} - S^{R,1}_{n,m}\right), \tag{4}$$

respectively. Similarly, the phase angle between the x and y components of the reference signal φ is calculated as [16]

$$\varphi = \frac{1}{2}\angle\left(S^{R,2}_{n,m} + iS^{R,3}_{n,m}\right). \tag{5}$$

Using these values the absolute values of the VTM elements are calculated as

#168000 - $15.00 USD Received 4 May 2012; revised 15 Jun 2012; accepted 16 Jun 2012; published 29 Jun 2012

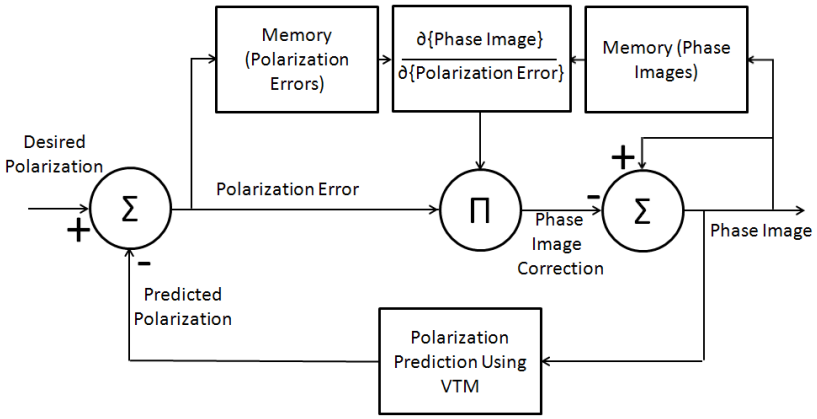

Fig. 2. A simplified block diagram outlining the procedure followed in calculating the phase image for polarization optimization. A given phase profile is changed iteratively until the polarization predicted by the VTM corresponding to the phase profile is similar to the desired polarization. At each iteration, corrections to the phase image are calculated based on both the nature of the change in polarization error and the phase image from previous iterations.

$$t_{n,m}^{xj} = \frac{T_{n,m}^{xj}}{\sqrt{I_{n,m}^{Rx}}}, \tag{6}$$

and

$$t_{n,m}^{yj} = \frac{T_{n,m}^{yj}}{\sqrt{I_{n,m}^{Ry}}} e^{i\varphi}, \tag{7}$$

where we take the phase of the x component of the reference signal as the datum for all of the phases involved in the experiments. As has been shown previously [2,6], controlling only intensity through the HSM does not require determination of the absolute value of the TM elements. However, for control of the polarization state, it is necessary to be able to tune the relative weights of the polarization components along basis states both in terms of the amplitude and phase, thus knowing the VTM elements to within a scaling factor only is of limited use. In addition, even for intensity only control, knowing the absolute values of the TM or VTM elements can facilitate quantitative control on the intensity, e.g., delivering a specified amount of light to a particular optical mode.

3. Phase image calculation for polarization control

The VTM of an HSM captures the medium's polarization changing behavior, and thus it is possible to predict the output polarization given the phase profile at the input. This ability can be used to calculate the phase image to be displayed on the NLC-SLM that can result in the desired polarization components at the output. To calculate the required phase profile, one can do a direct matrix inversion of Eq. (1). However, in general, it results in a required input field which can be realized only through both the phase and amplitude modulation of the input field-a capability which is not present in our current setup (we use a phase only SLM in the setup). In a similar situation, in intensity only studies [2], the results of the inversion have been

#168000 - $15.00 USD Received 4 May 2012; revised 15 Jun 2012; accepted 16 Jun 2012; published 29 Jun 2012

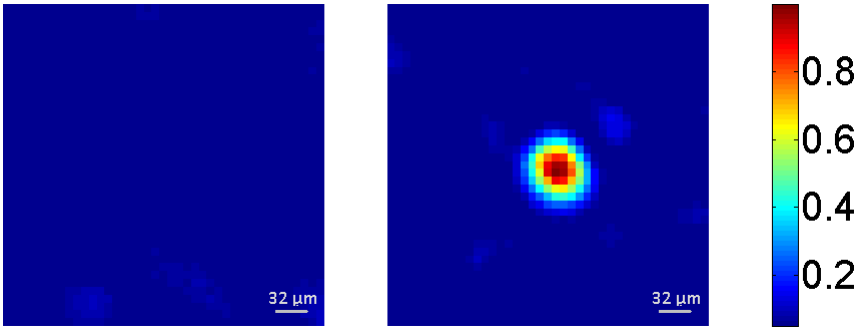

Fig. 3. Speckle field before and after optimization. An enhancement of 41× was observed with 256 control segments.

normalized. However, that cannot be done for polarization control as the type of normalization performed in [2] would change the relative strength of the orthogonal polarization components resulting in a polarization state different from the desired one. Thus, we resort to an iterative optimization process to calculate the phase image. A conceptual block diagram describing the basic steps in the calculation of the phase image is shown in Fig. 2. The process starts with a given phase image. Using the VTM the output polarization for the given phase image is predicted. The error between the desired and the predicted polarization is evaluated and is used to control the correction factor to be applied to the phase image. The nature of the change in errors as a function of phase images obtained from previous iterations determines the nature of the correction to be applied to the phase image.

Although Fig. 2 illustrates the concept, the actual steps followed in the optimization process are more complicated. Rather than optimizing for the polarization itself, we optimize for the intensity under the constraint that the predicted polarization be close to the desired polarization within a given tolerance limit. In our calculations, we characterize the polarization by the complex polarization ratio defined by two parameters: ϕ and R. These parameters are defined as the difference between the phase and the ratio of the magnitudes of the y and x polarization components, respectively [16]. The optimization problem to be solved is depicted in Eq. (8) and is solved by using the *interior point method* available in the KNITRO [19] optimization package accessed from MATLAB. As in any interior or barrier method, KNITRO breaks the optimization problem into a set of barrier sub-problems controlled by a barrier parameter. The algorithm then repeats the process of solving the sub-problem and reducing the barrier parameter until the optimization problem is solved [19].

$$\underset{\angle E_m^{i(I)}}{Maximize}\ I\left(\angle E_m^{i(I)}\right) subject\ to \begin{cases} \left| R^2 - \frac{\left|\sum E_n^{y(O)}\right|^2}{\left|\sum E_n^{x(O)}\right|^2} \right| < \varepsilon_r \\ \left(\phi - \angle\sum E_n^{y(O)} + \angle\sum E_n^{x(O)}\right) \mod 2\pi < \varepsilon_p \end{cases} . \tag{8}$$

We note that the iterative optimization followed in our case is a purely computational process as we utilize the information about the HSM contained in the VTM only. This approach is in contrast to the iterative optimization process followed, for example in [1] for intensity control, where one has to physically measure the intensity corresponding to each phase profile.

#168000 - $15.00 USD Received 4 May 2012; revised 15 Jun 2012; accepted 16 Jun 2012; published 29 Jun 2012

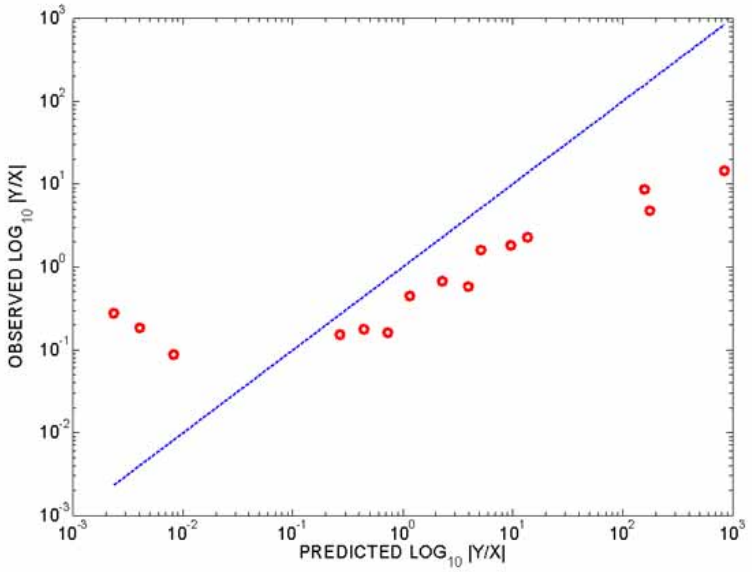

Fig. 4. Plot of the observed versus predicted polarization state to illustrate the value of the vector transmission matrix in predicting the output polarization state.

4. Results and discussion

To elucidate the usefulness of the VTM in predicting the polarization of the light focused through an HSM we carried out a series of experiments. The VTMs were at first measured and then used to design phase images that would focus light through the HSM. Initially, the optimization of the intensity of the focused light was carried out without considering the polarization information contained in the VTMs. Figure 3 shows a representative speckle pattern before and after optimization. For 256 control segments on the NLC-SLM, we were able to achieve an intensity improvement of more than 40$\times$ which is consistent with what has been previously reported in the literature using a similar number of control segments [2]; however, for basic polarization studies an improvement by a factor of 10$\times$ was found sufficient. Once the light was focused, the predicted output polarization of the phase image that resulted in the focused light was then calculated by using the VTM and compared with the actual polarization observed. The reference signal is blocked during the assessment of the observed polarization state.

A scatter plot of the observed versus predicted ratio of the intensities of the y and x polarization components have been plotted in Fig. 4. The diagonal line represents the ideal case of equal values of the predicted and the observed ratios and is shown for reference. Any deviation of the observed points from the diagonal line represents the error in the observed values. From the results we see that the observed ratios follow the predicted ratios to a large extent. The values are specially close for ratios between 0.1 and 10. For these ratios, the average relative error is 66%. Note that when the predicted ratios are too large or small, the observed ratios do not follow the predicted values as faithfully. We expect that this behavior stems from the interplay between the non-ideal experimental conditions, e.g., diffraction at the NLC-SLM, decorrelation of the system, error in the measurement of the characterstics of the reference signal and the stringent requirment on the accuracy of the model of the system when the ratios are too large or small.

#168000 - $15.00 USD Received 4 May 2012; revised 15 Jun 2012; accepted 16 Jun 2012; published 29 Jun 2012

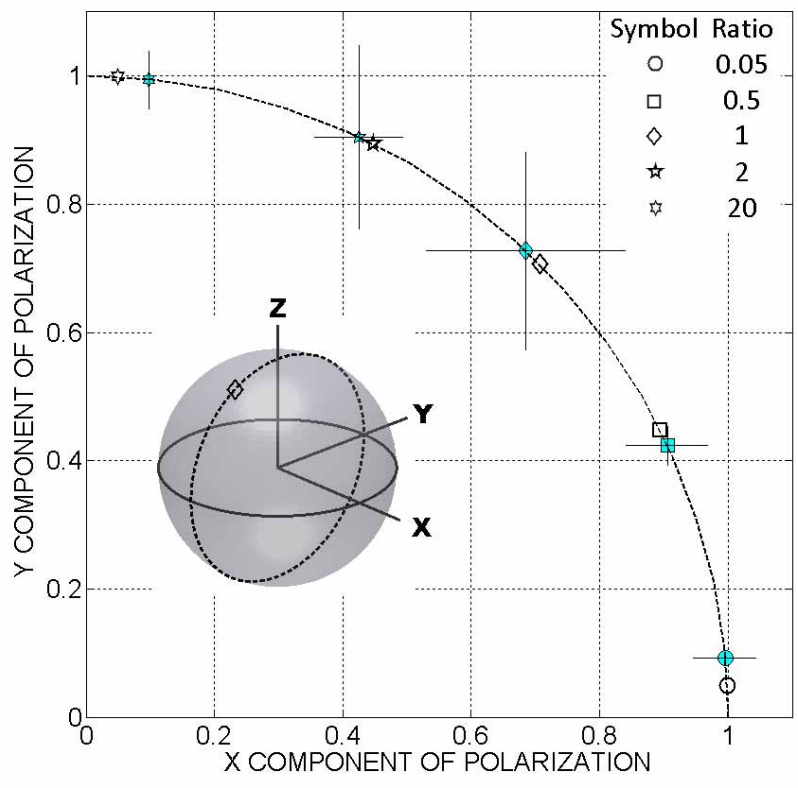

Fig. 5. Plot comparing the experimentally obtained (closed markers) and targeted (open markers) ratios of the intensities of the polarization components *y* and *x*. The dashed curve shows the trajectory of all possible ratios. Each ratio can represent any point on a unique circle on the Poincaré sphere; the inset shows the circle corresponding to the targeted polarization ratio of 1 outlined on the sphere.

Using the procedure outlined in Section 3, we calculated the phase images that would result in the ratios of 0.05, 0.5, 1, 2, and 20 for the intensities of the *y* and *x* polarization components. These phase images were then displayed on the NLC-SLM to modify the phase profile of the light incident on the HSM. The strength of the *x* and the *y* components of the focused light was then measured through the Stokes vector measurement. Due to the fact that our system had a speckle decorrelation time of $\sim$1 hr, the experiments were repeated with different sets of VTMs and different observation points. This is equivalent to repeating the experiment for different samples. For each desired ratio, the intensities of the measured *x* and *y* polarization components were normalized by the total intensity then plotted on the *xy* coordinate plane along with the standard deviations along the *x* and *y* directions. The results are shown in Fig. 5. The targeted values and the trajectory of all possible ratios is also shown for reference. Comparing the targeted and observed values we see that the observed values again follow the targeted ones.

Here we note that in Fig. 5 the trajectory of all possible ratios maps an arc of a unit circle in the first quadrant of the *xy* coordinate plane. Since the ratios of the *y* and *x* values change nonlinearly along the circumference of a circle, the plot has a nonlinear scale for the ratios. Note that due to the nonlinear nature of the scale, the large error bars for ratios near one do not signify large relative error compared to that for very small or very large ratios. Moreover, in our

#168000 - $15.00 USD Received 4 May 2012; revised 15 Jun 2012; accepted 16 Jun 2012; published 29 Jun 2012

experiments the available input degrees-of-freedom was found to be insufficient to control both the relative phase and intensities of the polarization components which limited us to exploring the control of the relative intensities only. Since the relative phases were neglected, each point shown in Fig. 5 could represent any point on a unique circle on the Poincar*é* sphere whereby the locus of a polarization with fixed intensity ratio is a circle normal to the x-axis. The inset in Fig. 5 shows a Poincar*é* sphere with the dashed circle corresponding to an intensity ratio of 1 outlined on it. We are working on modifying the experimental setup to allow for amplitude modulation at the input which we expect to facilitate finer control over the input field and help us explore the complete state of polarization control of the light focused thorough the highly scattering medium .

5. Conclusion

We presented a vector transmission matrix for the study of the polarization behavior of light propagation in highly scattering media. For M input field control segments and N observation points, the size of the vector transmission matrix is $2N \times 2M$ whereas the size for a scalar transmission matrix with the same number of input field control segments and observation points is $N \times M$. We also discussed a method for experimentally measuring the absolute values of the elements of the vector transmission matrix. The polarization behavior of the highly scattering media encoded in these elements was shown to be useful in predicting the magnitude of the complex polarization ratio of the light focused through such media. It was further shown that it is possible to calculate a phase profile for the light incident on the highly scattering medium that would deliver the desired magnitude of the complex polarization ratio at the targeted observation point. We are working on refining our experimental technique to extend our control to the phase of the complex polarization ratio which is necessary to exercise the complete control over the sate of polarization of the transmitted light. The ability to predict and control the polarization of the light transmitted through the highly scattering media has potential to be useful in a wide range of imaging, metrology, and fabrication problems.

Acknowledgments

We acknowledge financial support from the National Academies Keck Futures Initiative (NAS NAKFI IS10). S.T. and K.C.T. also acknowledge partial support from an NSF CAREER award (NSF DBI 09-54155).

#168000 - $15.00 USD Received 4 May 2012; revised 15 Jun 2012; accepted 16 Jun 2012; published 29 Jun 2012